



UNIVERSITY OF LEEDS

This is a repository copy of *Formation of wax walled microcapsules via double emulsion using cross membrane emulsification at elevated temperatures*.

White Rose Research Online URL for this paper:  
<http://eprints.whiterose.ac.uk/151280/>

Version: Accepted Version

---

**Article:**

Collins, S, York, DW [orcid.org/0000-0003-4778-3607](https://orcid.org/0000-0003-4778-3607), Kazmi, S et al. (1 more author)  
(2020) Formation of wax walled microcapsules via double emulsion using cross membrane emulsification at elevated temperatures. *Journal of Food Engineering*, 269. ARTN: 109739. ISSN 0260-8774

<https://doi.org/10.1016/j.jfoodeng.2019.109739>

---

© 2019 Elsevier Ltd. Licensed under the Creative Commons Attribution-NonCommercial-NoDerivatives 4.0 International License (<http://creativecommons.org/licenses/by-nc-nd/4.0/>).

**Reuse**

This article is distributed under the terms of the Creative Commons Attribution-NonCommercial-NoDerivatives (CC BY-NC-ND) licence. This licence only allows you to download this work and share it with others as long as you credit the authors, but you can't change the article in any way or use it commercially. More information and the full terms of the licence here: <https://creativecommons.org/licenses/>

**Takedown**

If you consider content in White Rose Research Online to be in breach of UK law, please notify us by emailing [eprints@whiterose.ac.uk](mailto:eprints@whiterose.ac.uk) including the URL of the record and the reason for the withdrawal request.



[eprints@whiterose.ac.uk](mailto:eprints@whiterose.ac.uk)  
<https://eprints.whiterose.ac.uk/>

**Formation of wax walled microcapsules via double emulsion using cross membrane emulsification at elevated temperatures**

Stephen Collins, David W. York, Sajid Kazmi and Akber Kaleem  
Mohammed

School of Chemical and Process Engineering, University of Leeds, Leeds LS2 9JT, UK

Corresponding author

Dr Stephen Collins

School of Chemical and Process Engineering, University of Leeds, Leeds LS2 9JT, UK

Email [mtlsc@leeds.ac.uk](mailto:mtlsc@leeds.ac.uk)

# **Formation of wax walled microcapsules via double emulsion using cross membrane emulsification at elevated temperatures**

## **Abstract**

A novel micro encapsulation process has been developed via a double emulsion of water in oil in water, whereby the oil is molten during the process and is then solidified to form a solid wall afterwards. This has the potential for an improved encapsulation technique for hydrophilic components. A range of materials was used, including hexadecane, lanolin and cetyl palmitate. Temperature controlled, cross membrane emulsification was used to ensure a narrow size distribution. Calculations of permeability, based on the leakage of fluorescein solutions, indicated a much higher rate that would be expected from such a hydrophobic, crystalline wall. Faster cooling gave rise to higher permeability. These suggest that pores are forming in thin walls during the solidification process and indicate the importance of process conditions on wall formation. Osmotic pressure differences are also a potential contributor.

Keywords: double emulsions, wax, microcapsule, permeability, cross membrane emulsification, flavour

## **Highlights**

- Cross membrane emulsification equipment has been modified to produce single and double emulsions in a controllable manner up to 95°C
- Emulsions obtained with waxes of elevated melting points including lanolin and beeswax
- Starting with W/O primary emulsions enabled ((W/O)/W) double emulsions to be obtained, which after cooling formed a solid shell

- The difference in leakage properties is not due to the thickness of the wax wall but the structure of the capsule wall

## **1. Introduction**

Flavour plays an important role in consumer satisfaction and influences further consumption of foods (Madene et al. 2006). In addition, food additives such as vitamins often need their taste masking to be palatable. To limit aroma degradation and loss during processing and storage, it is beneficial to encapsulate volatile ingredients prior to use.

Microencapsulation is a very versatile technology. The ability to control important properties such as stability, release rate and trigger mechanism, aesthetics and wall types makes it an attractive technology for all sorts of applications.

The development of microencapsulation products started in the 1950s with carbonless paper (Green and Schleicher 1956) and has since expanded to include cancer drugs (Higashi and Setoguchi 2000), flavours (Castro et al. 2016, Madene et al. 2006), food components (Ray et al 2016), cosmetic products (Carvalho 2016), fragrances (Teixeira et al. 2012), mosquito-repellent (Solomon et al. 2012) and insecticide (Hirech et al. 2003). In addition there is a wide range of wall materials as well as synthesis techniques. These include polymeric (Pan et al. 2013), and inorganic (Wang et al. 2008) walls, as well as the more recent development of metal walls (Hitchcock et al. 2015) and composites (Long et al. 2013) - all with their own properties. However, the applications of micro encapsulation is a small fraction of the options available. This is due to the restrictions that limit potential technologies. Of these the most important include:-

- Size of the material to be encapsulated, which limits the ability of the wall material to control diffusion across the shell. Thus, colloidosomes can hold in very large materials, such as bacteria but not small materials such as perfumes (Williams et al. 2012).
- Chemical compatibility of the active component with the process conditions and shell chemistry. Thus, chemicals with amine functionality will not survive a complex coacervation process that uses acid chlorides.
- Release mechanism will determine the material used for the shell. The shell material must be able to change its properties under the desired release condition. Often this release condition will vary so the release mechanism should be robust. Possible triggers include temperature (Bysell et al. 2011), mechanical action (Teixeira et al. 2012), biodegradation (Ramazani et al. 2016), and pH (Cayre et al. 2012).
- For a number of applications the shell material must not contain any harmful materials. Thus, for walls made by reactive components there should be no unreacted materials left and, for food applications all the materials should be food grade.
- Encapsulation is not a cheap process, especially for the more complex wall materials and processes. Thus, in practice encapsulation is limited to high value components with low usage levels (Madene et al. 2006, Milanovic et al. 2010).
- There is a further complication in that certain animal derivatives may not be acceptable to certain groups e.g. vegans

Natural waxes, such as beeswax and plant waxes (eg candelilla and carnauba) are available in food grade quality and are permitted in the European Union (E901-903). The use of wax as an encapsulation coating material has been investigated (Mellema et

al. 2006, Milanovic et al. 2010, Stojakovic´et al 2012). Mellema et al. (2006) used a mixture of active ingredient and molten wax (beeswax and PGPR) which was then formed into drops by deposition of hot wax with the functional ingredient on a plate, or by injection of hot wax with a (model) functional ingredient in cold oil while stirring with a high-shear mixer. Neither methods were controlled processes, not least in controlling the thickness of wall coating. In addition, the particles were relatively large 0.1 – 1 cm, or 150-500 µm depending on the method used. Nor was there any consideration given that the improvement could have been primarily due to reduced surface area:volume ratio through particle size enlargement. Milanovic et al. (2010) and Stojakovic´et al (2012) encapsulated vanillin (10% w/w) into carnauba wax. The size distribution was found to be bi-modal with main fraction in the range 210-360 µm and a small second shoulder representing large microparticles of sizes above 500 µm (Milanovic et al. 2010). They commented that further work was required in order to reduce particle size.

There are a number of different techniques used for encapsulation, including spray drying, spray-chilling, complex coacervation and melt dispersion (Madene et al. 2006, Milanovic et al. 2010). Spray dryers are common in the industrial sector but it is often difficult to control particle size (Milanovic et al. 2010). It is important to limit the maximum particle size, in food products such as spreads, to below 40 µm to avoid unpleasant feel in the mouth, while the smallest solid particles that can be sensed are 22 µm (Milanovic et al. 2010).

Membrane emulsification is a technique that produces emulsion droplets through extrusion of one liquid phase through micropores in a membrane into a second liquid phase (Williams et al. 2010). The use of membranes to manufacture emulsions and

other soft and hard particulates such as microcapsules can achieve a high degree of size control and consistency.

In cross-flow membrane emulsification (XME) the continuous phase is forced to flow across the membrane surface as shown in Figure 1. A pressure is applied to the disperse phase which forces it to permeate the membrane pores and form disperse phase droplets on the inner surface of the membrane in the path of the flowing continuous phase. The shear force caused by the cross flowing assists in the detachment of the droplets formed into the continuous phase.

The objectives of our work were to develop an improved encapsulation technique for hydrophilic ingredients by using a double emulsion where the aqueous component is formed into a water in oil emulsion using a wax above its melting point. This is then turned into a double emulsion in a further water environment and then cooled to solidify the droplets and produce a core shell material. By using a custom developed cross membrane emulsifier that can operate at 95°C good control of the various emulsion sizes can be obtained with no loss of the first emulsion and with a cost effective food grade material that is easy to scale up.

## **2. Experimental**

### **2.1 Chemicals**

Castor oil (Fluka), cetyl palmitate (Cutina CP) (BASF), fractionated coconut oil (Statfold Oils), Decon90 (Decon), fluorescein sodium salt (Sigma Aldrich), anhydrous lanolin (Fisher), mineral oil (light) (Sigma Aldrich), hexadecane 99% (Sigma Aldrich), polyglycerol polyricinoleate (PGPR 4150) (Palsgaard), sodium dodecyl sulphate (SDS) (GPR grade) (Fisher), Span80 (Sigma Aldrich), toluene (Sigma Aldrich), Tween20 (Fisher), white bees wax (PhEur) (Seatons), deionised water (Elix, Millipore), tap water,

and oxygen free nitrogen (BOC) were used as received.

## **2.2 Emulsification methods**

### 2.2.1 Rotor-stator homogenisation

A POLYTRON PT2100 (Kinematica) mini homogeniser was used for preparing small samples of single (W/O) emulsions. A larger rotor-stator homogeniser Ultra Turrax T25 Basic (IKA-WERKE) was used to prepare primary water in oil emulsions.

### 2.2.2 Cross flow membrane emulsification (XME)

An existing pilot plant XME instrument (Williams et al. 1998), which was capable of producing emulsions at room temperature was modified, to operate at least up to 95°C by the addition of appropriate heaters and controls (Fig 2).

A hydrophilic ceramic membrane (Ø 20 x 600mm) (Mantec Filtration) with 7 star-shaped channels and a mean pore size of 0.2 or 3 µm having an effective internal surface area of  $7.308 \times 10^{-2} \text{ m}^2$  was used. For all the runs the disperse phase was started second (i.e. the gas pressure was applied to the membrane after the aqueous phase was set to circulate). The gas used to provide the gas pressure was oxygen free nitrogen (BOC) at a pressure of 0.3MPa. After each run, the membrane was cleaned using a multi-stage process: ~5% Decon 90 at a specified flow rate with toluene; 5% Decon 90 at a specified flow rate and gas (empty oil phase); water at a specified flow rate and gas (empty oil phase). This last stage was repeated, usually three times, until the water was clear after being circulated. The flow rate used for cleaning was the same as that used in the XME run. The pressure used for cleaning was the same as that used in the XME run, 0.3MPa.

## 2.3 Emulsions prepared

### 2.3.1 Preliminary experiments

Oil in water (O/W) emulsions were prepared using two different methods. a) a POLYTRON PT2100 mini homogeniser was used at 26,000rpm for 1 minute to prepare oil in water emulsions of castor oil (10g water, 1.4g castor oil, 0.1g SDS) and coconut oil (10g water, 2g coconut oil and 0.2g SDS); b) XME was used to prepare oil in water emulsions of castor oil and coconut oil (as per Table 1).

### 2.3.2 Development heated XME

To test out the system at elevated temperatures, oils which are liquid at room temperature were used in the XME first to prepare oil-in-water emulsions. Two series of runs were performed (Table 1). The first series involved using mineral oil at 60-80°C (Mineral Oil 1 – 4) and using a membrane with a pore size of 0.2 and 3µm. The second series involved using mineral oil at 95°C (Mineral Oil 5), lanolin at 60°C (Lanolin 1) and beeswax at 80°C (Beeswax 1), each using a membrane with a pore size of 0.2 µm.

### 2.3.3 Double emulsions

The primary emulsions (W/O) of oil, water and fluorescein was prepared using a Ultra Turrax T25 Basic rotor-stator homogeniser at 9500rpm for 5min to ensure good mixing. A ratio of 2:3 of water to oil was used.

The concentrations of surfactant used were determined from stability tests where the stability of a range of surfactant concentrations was observed over time. For each test a series of samples were prepared which consisted of 2g oil, 3g water and varying percentages of PGPR surfactant (0, 0.5, 1, 2, 4 and 8%) (hexadecane and lanolin wrt oil, cetyl palmitate wrt to water). The emulsions were obtained using a POLYTRON PT2100 mini homogeniser at 26,000rpm for 1min. Figure 3 shows the emulsions over

time (1hr, 24hr, and 48hr). The minimum concentration required for the emulsions to remain stable after 48hr was: 1% for hexadecane, 4% for cetyl palmitate and 8% for lanolin.

For, hexadecane, the primary emulsion (W/O) was made using 200ml water, 0.3g fluorescein, 20g PGPR and 300ml (232g) hexadecane. For cetyl palmitate, the primary emulsion (W/O) was made using 200ml water, 0.3g fluorescein, 8g PGPR and 300ml (297g) of cetyl palmitate. For lanolin, the primary emulsion (W/O) was made using 200ml water, 0.3g fluorescein, 16g PGPR and 300ml (297g) of lanolin.

The double emulsions ((W/O)/W) were prepared using XME and the primary emulsions with conditions given in Table 1. The aim was to use a ratio of 1:2 primary emulsion to water but only cetyl palmitate went to completion (ie when all of the primary phase is converted into double emulsion).

Portions of each double emulsion ((W/O)/W) were placed in a 500ml beaker, open topped, and cooled in a variety of environments (freezer (-26°C), fridge (3°C) and room temperature (17-20°C)) with or without stirring, before performing size analysis and leakage tests.

## **2.4 Characterisation of emulsions**

Size analyses were performed using a Malvern Mastersizer 2000 (Malvern Instruments) in a Hydro S dispersion cell. Most emulsion samples were dispersed in deionised water using a dispersion cell before being stirred and pumped at 1750 rpm through the measurement cell. Primary emulsions (W/O) of hexadecane, cetyl palmitate and lanolin were dispersed in hexane. The scattering pattern obtained is deconvoluted (to produce the particle size distribution) using Mie theory. The refractive index and absorption of the sample applied in these calculations are 1.4 and 0.001 for mineral oil, 1.54 and 0.01

for coconut oil, 1.49 and 0 for castor oil, 1.434 and 0 for hexadecane, 1.442 and 0 for cetly palmitate, 1.44 for beeswax and 1.48 for lanolin. The refractive index of the dispersant is taken as 1.33 for water and 1.375 for hexane.

The amount of sample used was adjusted such that an obscuration of approximately 10% was obtained. Each sample was examined in three repeat measurement runs where each run consisted of ten separate measurements. Background and sample measurement times were 20 and 10 seconds, respectively. The average results of these multiple measurements are reported. The results are accurate up to  $\pm 1\%$ .

In addition to light scattering, an image analysis method was applied to examine the morphology of the emulsions. A flow-type histogram analyser, was used to examine the morphology of a large quantity of individual particles. The equipment, Sysmex FPIA-2100, combines flat sheath flow formation technology and image processing technology to analyse the particle images in the range of 0.6  $\mu\text{m}$  to 180  $\mu\text{m}$ . The equipment was calibrated using a standard 2  $\mu\text{m}$  latex sample.

The viscosity of the emulsions was not measured as it is not the objective of the research although incidental visual differences are reported here.

## **2.5 Leakage test**

Double emulsion ((W/O)/W) (15-16g) (after cooling in freezer ( $-26^{\circ}\text{C}$ ), fridge ( $3^{\circ}\text{C}$ ) or at room temperature ( $17-20^{\circ}\text{C}$ )) was poured into dialysis-tubing (M.W. 8000) and the dialysis tubing suspended in a beaker containing deionised water (250ml). The water was kept stirring using a magnetic stirrer and the absorbance of fluorescein in the water was measured at periodic intervals of time. The pore size of the dialysis tubing is such that only small molecules eg fluorescein, water can go through whilst capsules/emulsion droplets are retained.

## **2.6 UV/visible spectroscopy**

The leakage of fluorescein was measured at 490nm at periodic intervals of time using an Agilent 8453 Diode Array UV/VIS Spectrophotometer. The absorbance data was converted to concentration using a calibration curve according to Beer Lambert's law.

## **2.7 Differential Scanning Calorimetry**

The melting points of various waxes (lanolin, beeswax) were determined using a Perkin Elmer DSC 8000 scanning from 10 to 150°C under nitrogen at 10°C/min. The results were lanolin (39.19°C), and beeswax (64.20°C). Values from the suppliers were used for cetyl palmitate (dropping point 46-51°C) and hexadecane (melting point 18°C).

# **3. Results**

## **3.1 Preliminary experiments**

Membrane emulsification technology is robust in producing uniform size-predefined emulsion droplets from different disperse phases with very low to very high viscosity (Williams et al. 2010). The distinguishing feature is that the droplet size is controlled primarily by the choice of membrane and not by the generation of turbulent droplet break up (Joscelyne and Trägårdh 2000).

In cross-flow membrane emulsification (XME) the continuous phase is forced to flow across the membrane surface (Figure 1). A pressure is applied to the disperse phase which forces it to permeate the membrane pores and form disperse phase droplets on the inner surface of the membrane in the path of the flowing continuous phase. Droplets grow at pore outlets until, on reaching a certain size, they detach (Joscelyne and Trägårdh 2000). This is determined by the balance between the drag force on the droplet

from the flowing continuous phase, the buoyancy of the droplet (which is very small (Peng and Williams 1998)), the interfacial tension forces and the driving pressure (which is constant in all the XME runs presented (Section 2.2.2)).

Figure 4 compares the size distribution of two (O/W) emulsion systems prepared by cross-flow membrane technology (with 0.2 $\mu$ m membrane) and rotor-stator homogenization (26,000rpm). For coconut oil (Fig 4a) the high speed mixer produces a broad range of particles (peak  $\sim$ 15  $\mu$ m) whilst the XME produces particles with a narrower range and smaller average particle size (peak  $\sim$  2.5 $\mu$ m). For castor oil (Fig 4b) the high speed mixer also produces a broad range of particles (peak  $\sim$ 40  $\mu$ m) whilst the XME produces particles with a narrower range and smaller average particle size (peak  $\sim$  0.7 $\mu$ m).

These experiments highlight the disadvantages of rotor/stator high shear mixers and high - pressure homogenisers, namely that droplet size and size distribution are not well controlled (Spyropoulos et al 2011). In addition such mechanical methods require large inputs of energy and subject the emulsions to high shear and thermal stresses which may have undesirable consequence on sensitive ingredients such as proteins (Spyropoulos et al 2011). In contrast, membrane emulsification (such as XME) produces emulsion droplets individually/one-at a time which enables size and size distribution to be carefully controlled along with lower levels of shear and lower energy demands (Peng and Williams 1998, Spyropoulos et al 2011).

The XME (Figure 4) produced peaks larger than the average pore size. This occurs as the droplet grows on the membrane surface until the droplet is big enough to be carried away by the shear forces of the continuous phase. The ratios of particle size to pore size found here (12.6 for coconut oil and 3.6 for castor oil) compare well with reported ratios in the range of x2 or sometimes up to more than x10 (Williams et al.

2010, Spyropoulos et al. 2014). In addition, the difference between the flux for castor oil (4.2 ml/min) and coconut oil (22.2 ml/min) (Table 1) can be attributed to the difference in their viscosity (Williams et al. 2010).

### **3.2 Development of heated XME**

One of the major potential advantages of XME is the scale-up capability for large scale industrial operations. A pilot-scale XME plant (Williams et al. 1998) was adapted to enable heating of the system to at least 95°C by the addition of electric heaters at appropriate places and associated electronic control instrumentation (Figure 2). Mineral oil was used to test out the capability of the modified XME as it is a liquid at room temperature, meaning that if the temperature control modification failed the XME would not end up blocked with a solidified wax.

Mineral oil was used using ceramic tubes with an average pore size of 0.2 and 3  $\mu\text{m}$ , at temperatures of 60 and 80°C. Using a membrane with average pore size 0.2  $\mu\text{m}$  produced (Figure 5a) two peaks – a main one ( $\sim 0.8 \mu\text{m}$ ) and a minor one ( $\sim 0.1 \mu\text{m}$ ) (which previous experience has shown to be an artefact). The ratios of particle size to pore size found here ( $\sim 4$ ) is in the range found earlier (Section 3.1). Increasing the temperature from 60 to 80°C had little effect on the size distribution whilst an increase in the flux was obtained (9.8 ml/min at 60°C compared with 26.0 ml/min at 80°C) (Table 1), as expected (Williams et al. 2010).

Using a membrane with average pore size 3  $\mu\text{m}$  produced two peaks whose size distribution varied with the temperature used (Figure 5b). With 60° C, the main peak was 15 $\mu\text{m}$  and the minor one  $\sim 0.7\mu\text{m}$ , whilst for 80°C the main peak was 45 $\mu\text{m}$  and the minor one  $\sim 0.6\mu\text{m}$ . Most runs had constant flow rate of the continuous phase but these runs had a lower flow rate (200 l/hr for 3 $\mu\text{m}$  instead of 500 l/hr for 0.2 $\mu\text{m}$ ) (Table 10) and it is known that lower flow rate produces larger size droplets (Williams et al. 2010)

as the gentler flowing continuous phase exerts less shear force on the growing droplets giving them a longer time to grow before becoming detached.

The ratios of particle size to pore size found here (~7.5 - 15) is similar to the range found earlier (Section 3.1). Interestingly the minor peak is approximately the same as the main peak obtained using the 0.2 $\mu$ m membrane. The presence of two peaks is surprising as it would be expected that the mineral oil would behave as a single homogenous liquid and so produce one peak. As the minor peaks are smaller than the average pore size (3  $\mu$ m) then they may have arisen by some of the oil going straight through the membrane (“jetting”), which suggests that the transmembrane pressure for this system was slightly too high ( Peng and Williams 1998). Again there is an expected increase in the flux (Williams et al. 2010) (178.6 ml/min at 80°C compared with 38.7 ml/min at 60°C) (Table 1).

Comparing results from the different pore sizes (Figure 5 a,b, Table 1) indicates a number of similarities and differences. For each pore size, an increase in temperature increases the flux which is to be expected as the oil becomes more fluid. At the same time, the size distribution stays the same for the 0.2 $\mu$ m tube but changes for the 3 $\mu$ m tube. This may be because the droplets for the 0.2 $\mu$ m tube are growing close to the pore and have little flexibility to distort whilst growing, whilst the droplets from the 3 $\mu$ m tube are larger and have more room to deform/continue growing in higher temperature (lower viscosity) conditions.

### **3.3 Preparing O/W emulsions using waxes**

As the tests (Section 3.2) showed that the heating modifications to the XME worked then the next step of using waxes was undertaken (using a ceramic tube with an average pore size of 0.2  $\mu$ m) to produce O/W emulsions (Table 1) with the volume size

distributions shown in Figure 5c.

Lanolin (melting point 39°C) was used at 60°C with the O/W emulsion having two peaks: main one at 0.4 µm and smaller one at 4 µm. Bees wax (melting point 64°C) was used at 80°C with the O/W emulsion having two peaks: main one at 9 µm and smaller one at 0.3 µm.

To be doubly sure that the XME could cope with a range of waxes mineral oil was used again but at 95°C with the emulsion (Figure 5c) having two peaks: at 1.4 and 16 µm. The increase in the flux (90.9 ml/min at 95°C compared with 26.0 ml/min at 80°C and 9.8 ml/min at 60°C) (Table 1), can be attributed to the expected change in viscosity with temperature (Floros 2017) having an effect on the flux (Williams et al. 2010).

The presence of two peaks in these three emulsifications is surprising. To check whether the O/W emulsions were really discrete droplets, or the larger peak was caused by agglomeration of smaller sized droplets, or the droplets were elongated objects (where the two peaks represent length and width) the emulsions were examined using a Sysmex image analysis instrument. The results are in Table 2 which provides the number of particles in each size range and Figure 6 which gives a few of the images for each size range. (NB only some of the 11-15,000 particles analysed are shown.)

For lanolin (Figure 6), almost all of the particles are <5µm and these are discrete, mostly spherical. The few particles larger than 5µm tend to be agglomerates. For beeswax, most of the particles are <5µm and these are discrete, mostly spherical. Particles 5-10 µm in size tend to be a mix of discrete and agglomerates whilst those particles larger than 10µm tend to be agglomerates. For mineral oil (at 95°C) almost all of the particles are <5µm. Almost all the particles are discrete, and spherical. Only the occasional particle (<5%) is an agglomerate.

Comparing the image analysis data of double emulsions (Figure 6) with the volume size distributions (Figure 5c, Table 2) suggests that for a) lanolin that the main peak at 0.4  $\mu\text{m}$  is discrete droplets with the minor peak at 4  $\mu\text{m}$  arising from agglomeration of smaller particles; b) beeswax that the peak at 0.3  $\mu\text{m}$  is discrete droplets with the peak at 9  $\mu\text{m}$  arising from a mixture of discrete droplets and agglomeration of smaller particles; and c) mineral oil (at 95°C) suggests that the peaks at 1.4 and 16  $\mu\text{m}$  are almost all discrete droplets.

Droplets produced by XME are often reported to be of diameters a few times that of the pore size (Vladisavljević & Williams 2005, Nakashima et al. 2000) and these results fit that pattern. The use of higher concentrations of surfactant might reduce the agglomeration that has occurred. The concentration of surfactant used was decided by the result of stability tests (Section 2.2.3). These only provide an approximation of the surfactant required for XME, as stability tests use a standard homogeniser, which produce a different size range of emulsion droplets from that produced by XME (Section 3.1). However, it is still worthwhile using stability tests as a first approximation as they are much easier to perform than using XME, and allow for subsequent refining of the concentration later if necessary.

### **3.4 Wax walled capsules**

Having established (Section 3.3) that it was possible to make O/W emulsions using waxes, wax walled capsules were now prepared. Primary emulsions (W/O) of waxes (hexadecane (melting point = 18°C), lanolin (mp 39°C) and cetyl palmitate (mp = 46-51°C)) were prepared using a rotor-stator homogeniser and then converted into double emulsions ((W/O)/W) using XME.

It has been shown that cooling temperature has had an effect on the release of dye from wax and glyceride solid lipid nanoparticles by rapid cooling inducing recrystallization, and so making wax more ordered (Jenning & Gohla 2000). Consequently, molten droplets present in the double emulsion were cooled at three different temperatures (freezer (-26°C), fridge (3°C) and room temperature (17-20°C)) to form capsules. Fluorescein was incorporated into the primary wax emulsions to enable leakage properties to be determined of the capsules in the double emulsions. The initial rate of diffusion was determined by measuring the leakage rate over the first 180-360 min of leakage.

#### 3.4.1 Hexadecane

Primary emulsion (W/O) of hexadecane and water (3:2) containing fluorescein was prepared then the double emulsion ((W/O)/W) prepared using the primary emulsion and water (aim ratio 1:2) with average XME pore size of 0.2µm. The size distribution of the primary emulsion (Figure 7a) has a main peak ~11.5 µm with a shoulder around ~3.3µm, whilst the double emulsion (Figure 7b) has a main peak ~0.5µm and a minor peak ~2.5µm (Table 3). The size distribution is as expected when using XME, with the main peak being x2 the pore size of the membrane tube, which compares well with reported ratios (Williams et al. 2010). The minor peak at ~2.5µm may have arisen through some droplets coalescing.

Figure 8 shows the primary and double emulsions made using hexadecane. The fact that the double emulsion is much fainter in colour than the primary emulsion indicates that the fluorescein in the primary emulsion had been enclosed in the second emulsification step. Further study using SEM is necessary to conclusively prove that the resulting microcapsules are core shell.

The initial rate of diffusion of fluorescein was determined at room temperature from the double emulsion after it had been split into three and cooled under different cooling temperature conditions (-26°C, 3°C and 17°C) (Figure 9a) (Table 4). The rate of diffusion was greatest for -26°C, followed by 3°C followed by room temperature (17°C).

#### 3.4.2 Cetyl palmitate

Primary emulsion (W/O) of cetyl palmitate and water (3:2) containing fluorescein was prepared then the double emulsion ((W/O)/W) prepared using the primary emulsion and water (aim ratio 1:2) with average pore size 3µm. A larger sized pore size was used (compared with the 0.2µm for hexadecane) because of the increased viscosity of the cetyl palmitate emulsion as it is known that higher viscosity reduces flux (Williams et al. 2010) and the flux for the hexadecane emulsion was already low (0.9 g/min) (Table 1).

The size distribution of the primary emulsion (Figure 7c) has a main peak ~60.3 µm with a minor peak around ~8.7µm. Compared with the primary emulsion of hexadecane, the size distribution of cetyl palmitate primary emulsion droplets is considerably higher. This might be because cetyl palmitate has higher viscosity compared to hexadecane (cf the stirring speed of the homogeniser used was the same for both tests).

The double emulsion was split into three and cooled under three different temperature conditions (-26°C, 3°C and 20°C). As a consequence the emulsions solidified and were subsequently warmed in order to melt them so that their size distribution could be determined (Figure 7d). The three samples showed a similar size distribution with a main peak at ~35-46µm and two minor peaks (~0.3-0.4 and ~2-

4 $\mu\text{m}$ ). (Previous experience has shown that an artefact at 0.1 $\mu\text{m}$  is sometimes obtained using a tube with average pore size 0.2 $\mu\text{m}$ . Consequently, the peak at ~0.3-0.4 $\mu\text{m}$  here and for lanolin ((Section 3.4.3)) might be an artefact from the larger average sized tube (3 $\mu\text{m}$ ) used here.) Although the main peak is higher than for hexadecane it is still less than the primary emulsion of cetyl palmitate (main peak ~60 $\mu\text{m}$ ). The main reason for the larger double emulsion for cetyl palmitate would be that the XME tube used had a larger average pore size (3 $\mu\text{m}$ ) than was used for hexadecane (0.2 $\mu\text{m}$ ).

The initial rate of diffusion of fluorescein was determined at room temperature from the double emulsion after it had been split into three and cooled under three different temperature conditions (-26°C, 3°C and 20°C) (Figure 9b) (Table 4). The rate of diffusion was greatest for -26°C, followed by room temperature (20°C) followed by 3°C. Each was a magnitude higher than the rate for hexadecane.

### 3.4.3 Lanolin

Primary emulsion (W/O) of lanolin and water (3:2) containing fluorescein was prepared then the double emulsion ((W/O)/W) prepared using the primary emulsion and water (aim ratio 1:2) with average pore size 3 $\mu\text{m}$ . Figure 7e shows the size distribution of the primary emulsion (stirred whilst it was cooling). The primary emulsion has a main peak ~11.5  $\mu\text{m}$  (Table 3).

The double emulsion was split into three samples: i) this was not stirred whilst cooled at room temperature (20°C); ii) this was stirred whilst cooled at room temperature (20°C) – two layers formed – a creamy solid layer on top and bottom aqueous layer; and iii) this was stirred whilst cooled at 3°C (ice bath) – whilst measuring the size distribution, little lumps ~1-2mm were observed floating in the

sample. These lumps will have arisen through emulsion instability of the emulsion probably coalescence or Ostwald ripening (Binks 1998).

The size measurement results (Figure 7f) for double emulsion stirred whilst cooling at different temperatures (room temperature (20°C) and 3°C) show similar results. The sample cooled at 20°C has main peak at ~20µm (Table 3) and minor peak at ~0.3µm, whilst the sample cooled at 3°C had a main peak ~17.3µm and minor peak at ~0.3µm.

The non-stirred sample of double emulsion (cooled at room temperature) had separated into two layers: the top layer comprising double emulsion and the bottom layer comprising cloudy water. The top layer (Figure 7f) consisted of a single peak ~17.4µm (Table 3), whilst the bottom layer had a broader range of size distributions with main peaks at ~5.0 and ~17.4µm as well as 0.3µm (artefact) and ~182µm (possibly arising from coalescence). However, the bottom aqueous layer appears to have a much lower concentration so the overall proportion represented by the bottom layer is low.

The main reason for the larger size double emulsion of lanolin than hexadecane would again be that the XME tube used had a larger average pore size (3µm) than was used for hexadecane (0.2µm). Unlike hexadecane and cetyl palmitate where the average emulsion size decreased after going through the XME, for lanolin it increased, from ~11.5µm to ~20µm (Table 3). This maybe because lanolin is a complicated mix of esters plus some free acids and alcohols (Collins & Davidson 1997) resulting in a much more polar environment which encourages droplet growth on the membrane wall.

The duration of emulsification varied (Table 1) between hexadecane (165g in 180min, 0.2µm tube), cetyl palmitate (463g in 40min, 3 µm tube) and lanolin (209g in 120min, 3µm tube). The main difference in emulsion sizes between hexadecane and cetyl palmitate can be attributed to the difference in average pore sizes, which is

something already noted as being responsible for the difference in the size of the resulting double emulsion. However, for cetyl palmitate and lanolin, both using the same pore size tubes, the difference in emulsion sizes may be due to the difference in chemical composition affecting the interfacial tension forces during droplet growth.

The initial rate of diffusion of fluorescein was determined at room temperature from the double emulsion cooled under three different conditions (3°C (stirred), 20°C (stirred) and 20°C (non-stirred)) (Figure 9c) (Table 4). The rate of diffusion was greatest for 3°C (stirred), followed by 20°C (non-stirred) then 20°C (stirred). The rates were in between the values for hexadecane and cetyl palmitate.

#### 3.4.4 Discussion

A summary of the double emulsion leakage results is given in Table 4. The concentration gradient from the (initial) concentration versus time experiments was used as the diffusion rate (Table 4). Fick's Second Law (Equation 1) (Cussler 2009) was used to convert this into permeability:

$$P = [DH] = \frac{j_i l}{\Delta c} = \frac{\beta \left( \frac{dc}{dt} \right) * x}{\Delta c} \quad (1)$$

Where D is the rate of diffusion of fluorescein through the wax wall, H is the partition coefficient of fluorescein in wax wall,  $dc/dt$  is the measured diffusion rate,  $x$  is the wall thickness,  $\Delta c$ , is the initial difference in concentration across the capsule wall. and  $\beta$  is a physical constant containing the dimensions of the leakage cell and the dialysis tubing. We are assuming that the partition coefficient, H, is similar for the highly polar fluorescein, given the chemical similarity of the waxes, and so, the major differences in the results is due to diffusion rates (which are effected by the physical state of the wall and, in this case its porosity).

The wall thickness was calculated using the  $D[4,3]$  (which is the volume weighted mean) of the double emulsion as a measure of the average particle size (ie external double emulsion size), and the known composition:

$$\text{Radius of whole sphere} \quad R_W = \frac{D[4,3]}{2} \quad (2)$$

$$\text{Volume of whole sphere} \quad Vol_W = \frac{4\pi}{3} R_W^3 \quad (3)$$

$$\text{Radius of inner sphere} \quad R_I = \left( \frac{3}{4\pi} (0.4 Vol_W) \right)^{1/3} \quad (4)$$

$$\text{Thickness} \quad Thickness = R_W - R_I \quad (5)$$

Where 0.4 comes from the volume proportion of water in single emulsion, and assuming a perfect spherical core shell structure with wax as shell, for the solidified double emulsion.

The data for the change in fluorescein concentration over time for the double emulsion ((W/O)/W) samples has been replotted as  $C/C_0$  in order to allow for the effect of cooling temperature  $-26^\circ\text{C}$ ,  $3^\circ\text{C}$  and room temperature ( $17-20^\circ\text{C}$ ) (Figure 10) of the different double emulsions to be compared. (It should be noted that controlling the cooling temperature is not the same as precisely controlling the cooling rate.) For each cooling temperature the equilibrium level of concentration ( $C/C_0$ ) was lowest for hexadecane, with cetyl palmitate and lanolin being similar. This contrasts with the initial rate of diffusion (Table 4) where cetyl palmitate (mp  $46-51^\circ\text{C}$ ) had the highest rate of diffusion, followed by lanolin (mp  $39^\circ\text{C}$ ) with hexadecane (mp  $18^\circ\text{C}$ ) having the least. A similar pattern is observed with the permeability (Table 4) with permeability increasing with higher wax melting point: cetyl palmitate highest ( $195-2,530 \times 10^{-16} \text{ m}^2\text{s}^{-1}$ ), lanolin next ( $59-86 \times 10^{-16} \text{ m}^2\text{s}^{-1}$ ) and hexadecane lowest ( $2 \times 10^{-16} \text{ m}^2\text{s}^{-1}$ ).

It is not surprising that there is some difference between hexadecane and lanolin / cetyl palmitate for mean capsule size  $D[4,3]$  and wax thickness as XME tubes with

different average pore sizes were used (0.2 $\mu\text{m}$  for hexadecane and 3 $\mu\text{m}$  for lanolin/cetyl palmitate). Multiplying the D[4,3] for hexadecane (1.074  $\mu\text{m}$ ) by 15 (the ratio of the different pore sizes) produces a D[4,3] of 16.11 $\mu\text{m}$ . This corresponds to a wax thickness of 2.12 $\mu\text{m}$ , which is approximately the same as that for lanolin (Table 4), i.e. the range in permeability is not due to using different XME tube pore sizes, and there is a real difference between the different waxes.

For each wax (Table 4) there is an effect of cooling temperature on the permeability, with lower cooling temperature (-26°C) highest, then fridge (3°C) then room temperature (17-20°C). For a solid wall, permeability should be independent of wall thickness but the results show that the permeability varies with wall thickness (Figure 11), indicating that the walls are porous, and so related to the crystal structure of the capsule wall (Mellema et al. 2006). We hypothesise that the rate of cooling is impacting on the packing of the wax molecules in the wall and so on its porosity. This phenomena needs further investigation. Mellema et al. (2006) also postulates that one cause of the release could be due to osmotic pressure but this hypothesis has not been tested. It is difficult to access the exact magnitude of differing process conditions on the permeability of the walls formed. This is because there is little published data on the pure wax materials, something which is needed in order to understand wall packing, and which is addressed in our subsequent paper (York et al. 2019).

#### **4. Conclusions**

Cross membrane emulsification equipment has been modified to produce single and double emulsions in a controllable manner at temperatures up to 95°C, at a pilot plant scale. Emulsions were obtained with waxes of elevated melting points including

lanolin and beeswax. Using this equipment and starting with W/O primary emulsions enabled ((W/O)/W) double emulsions to be obtained, which after cooling formed a solid shell. Microcapsules were formed using hexadecane, lanolin and cetyl palmitate as hydrophobic wall materials.

For each cooling temperature, the permeability increased with higher wax melting point. For each wax the permeability was higher with lower cooling temperature. There is no obvious connection with the mean capsule size (D[4,3]) or the wall thickness.

Consequently, the difference in leakage properties is not due to the thickness of the wax wall but the structure of the capsule wall. We hypothesise that this change in permeability is likely due to variations in shell wall porosity as the waxes cool. More work is required to assess the cause of the higher than expected permeability.

### **Acknowledgments**

We wish to thank METRC Short Term Project Funding M9095 (“Novel processing of wax/silicone oil capsules”) for part funding of this project, and Mo Javed, SCAPE, University of Leeds for performing the DSC.

### **Disclosure statement**

No potential conflict of interest was reported by the authors.

### **References**

Binks B.P. (ed). (1998) Modern aspects of emulsion science. Royal Society of Chemistry, Cambridge

- Bysell H., Månsson R., Hansson P., & Malmsten M. (2011) Microgels and microcapsules in peptide and protein drug delivery. *Advanced Drug Delivery Reviews*, 63, 1172–1185.
- Carvalho I.T., Estevinho B.N., & Santos L. (2016) Application of microencapsulated essential oils in cosmetic and personal healthcare products – a review. *International Journal of Cosmetic Science*, 38, 109–119.
- Castro N., Durrieu V., Raynaud C., Rouilly A., Rigal L., & Quellet, C. (2016) Melt Extrusion Encapsulation of Flavors: A Review. *Polymer Reviews*, 56, 137–186.
- Cayre O.J., Hitchcock J., Manga M.S., Fincham S., Simoes A., Williams R.A., & Biggs S. (2012) pH-responsive colloidosomes and their use for controlling release. *Soft Matter*, 8, 4717-4724.
- Collins S., & Davidson R.S. (1997) Aspects of the photochemistry of wool yolk (wool wax and suint). *Review in Progress in Coloration*, 27, 42-58.
- Cussler E.L. (2009) *Diffusion: Mass Transfer in Fluid Systems* (3rd edition) Cambridge University Press, Cambridge.
- Floros M.C., Raghunanan L., Narine S.S., (2017) A toolbox for the characterization of biobased waxes. *European Journal of Lipid Science and Technology*, 119, 1600360
- Gasparini G., Kosvintsev S.R., Stillwell M.T., & Holdich R.G. (2008) Preparation and characterization of PLGA particles for subcutaneous controlled drug release by membrane emulsification. *Colloids and Surfaces B: Biointerfaces*, 61, 199–207.
- Green B.K., & Schleicher L. (10 January 1956) Pressure responsive record materials US patent 2,730,457.
- Higashi S., & Setoguchi T. (2000) Hepatic arterial injection chemotherapy for hepatocellular carcinoma with epirubicin aqueous solution as numerous vesicles

in iodinated poppy-seed oil microdroplets: clinical application of water-in-oil-in-water emulsion prepared using a membrane emulsification technique. *Advanced Drug Delivery Reviews*, 45, 57–64.

Hirech K., Payan S., Carnelle G., Brujes L., & Legrand J. (2003) Microencapsulation of an insecticide by interfacial polymerisation. *Powder Technology* 130, 324-330.

Hitchcock J.P., Tasker A.L., Baxter E.A., Biggs S., & Cayre O.J. (2015) Long-Term Retention of Small, Volatile Molecular Species within Metallic Microcapsules. *ACS Applied Materials & Interfaces*, 7, 14808–14815.

Jenning V., & Gohla S. (2000) Comparison of wax and glyceride solid lipid nanoparticles (SLN). *International Journal of Pharmaceutics* 196, 219–222.

Joscelyne S.M., & Trägårdh G. (2000) Membrane emulsification—a literature review. *Journal of Membrane Science* 169, 107–117

Long Y., Song K., York D., Zhang Z., & Preece J.A. (2013) Engineering the mechanical and physical properties of organic–inorganic composite microcapsules. *Colloids and Surfaces A: Physicochemical and Engineering Aspects*, 433, 30–36.

Madene A., Jacquot M., Scher J., & Desobry S. (2006) Flavour encapsulation and controlled release – a review. *International Journal of Food Science and Technology*, 41, 1–21.

Mellema M., van Benthum W.A.J., Boer B., von Harras J., & Visser A. (2006) Wax encapsulation of water-soluble compounds for application in foods. *Journal of Microencapsulation*, 23(7), 729–740.

Milanovic J., Manojlovic V., Levic S., Rajic N., Nedovic V., & Bugarski B. (2010) Microencapsulation of Flavors in Carnauba Wax. *Sensors*, 10, 901-912.

- Nakashima T., Shimizu M., & Kukizaki M. (2000) Particle control of emulsion by membrane emulsification and its applications. *Advanced Drug Delivery Reviews*, 45, 47–56.
- Pan X., Mercadé-Prieto R., York D., Preece J.A., & Zhang Z. (2013) Structure and Mechanical Properties of Consumer-Friendly PMMA Microcapsules. *Industrial & Engineering Chemistry Research*, 52, 11253–11265.
- Peng S.J., & Williams R.A. (1998) Controlled Production of Emulsions Using a Crossflow Membrane Part I: Droplet Formation from a Single Pore. *Transactions of the Institution of Chemical Engineers Part A, Chemical Engineering Research and Design*, 76, 894-901.
- Ramazani F., Chen W., van Nostrum C.F., Storm G., Kiessling F., Lammers T., Hennink W.E., & Kok R.J. (2016) Strategies for encapsulation of small hydrophilic and amphiphilic drugs in PLGA microspheres: State-of-the-art and challenges. *International Journal of Pharmaceutics*, 499, 358–367.
- Ray S., Raychaudhuri U., & Chakraborty R. (2016) An overview of encapsulation of active compounds used in food products by drying technology. *Food Bioscience*, 13, 76–83.
- Solomon B., Sahle F.F., Gebre-Mariam T., Asres K., & Neubert R.H.H. (2012) Microencapsulation of citronella oil for mosquito-repellent application: Formulation and in vitro permeation studies. *European Journal of Pharmaceutics and Biopharmaceutics*, 80, 61–66.
- Spyropoulos F., Hancocks R.D., & Norton I.T. (2011) Food-grade emulsions prepared by membrane emulsification *Procedia Food Science* 1, 920 – 926
- Spyropoulos F., Lloyd D.M., Hancocks R.D., & Pawlik A.K. (2014) Advances in membrane emulsification. Part A: recent developments in processing aspects and

microstructural design approaches *Journal of the Science of Food and Agriculture*, 94, 613–627.

- Stojakovic´ D., Bugarski B., & Rajic´ N. (2012) A kinetic study of the release of vanillin encapsulated in Carnauba wax microcapsules. *Journal of Food Engineering* 109, 640–642
- Sun G., & Zhang Z. (2011) Mechanical properties of melamine-formaldehyde microcapsules. *Journal of Microencapsulation*, 18, 593-602.
- Teixeira C.S.N.R., Martins I.M.D., Mata V.L.G., Barreiro M.F.F., & Rodrigues A.E. (2012) Characterization and evaluation of commercial fragrance microcapsules for textile application. *Journal of the Textile Institute*, 103, 269–282.
- Vladislavljević G.T., & Williams R.A. (2005) Recent developments in manufacturing emulsions and particulate products using membranes. *Advances in Colloid and Interface Science*, 113, 1 – 20.
- Wang J-X., Wang Z-H., Chen J-F., & Yun J. (2008) Direct encapsulation of water-soluble drug into silica microcapsules for sustained release applications. *Materials Research Bulletin*, 43, 3374–3381.
- Williams M., Armes S.P., & York D.W. (2012) Clay-Based Colloidosomes. *Langmuir*, 28, 1142–1148.
- Williams R., Yuan Q., & Collins S. (2010) Membrane Emulsification, in *Encyclopedia of Surface and Colloid Science* (1: 1, 1 — 27) Taylor & Francis, London.
- Williams R.A, Peng S.J., Wheeler D.A, Morley N.C., Taylor D., Whalley M., & Houldsworth D.W. (1998) Controlled Production of Emulsions Using a Crossflow Membrane Part II: Industrial Scale Manufacture. *Transactions of the Institution of Chemical Engineers Part A, Chemical Engineering Research and Design*, 76, 902-910.

York D.W., Collins S., & Rantape M. (2019) Measuring the permeability of thin solid layers of natural waxes. *Journal of Colloid and Interface Science*, 551, 270-282.

Table 1. Recipes and experimental conditions used for the primary (W/O) and double ((W/O)/W) emulsions prepared using XME.

Table 2 Number of emulsion droplets in each size range for O/W emulsions prepared using XME of lanolin, beeswax and mineral oil obtained using image analysis with two different lens magnifications

Table 3 Size distribution results for primary (W/O) and double ((W/O)/W) emulsions of hexadecane, cetyl palmitate and lanolin prepared using XME (cooled at different temperatures).

Table 4 Properties of wax microcapsules prepared using primary emulsions of hexadecane, lanolin and cetyl palmitate

Figure 1. Schematic representation of cross flow membrane emulsification.

Figure 2. View of pilot scale XME rig from the rear, after modification (  = heated modification) where A = aqueous tank (continuous phase), O = organic phase (disperse phase), and X = XME tube

Figure 3 Photograph of primary emulsions (W/O) of oil (hexadecane, cetyl palmitate or lanolin) and water (ratio 2:3 water to oil) made using PGPR surfactant concentration of 0, 0.5, 1, 2, 4 and 8% (hexadecane and lanolin wrt oil, cetyl palmitate wrt to water) from left to right, monitored over time

Figure 4 Volume size distributions of oil-in water emulsions made using either XME or a high speed mixer with a) coconut oil and water, and b) castor oil and water

Figure 5 Volume size distribution of oil-in-water emulsions as a function of operating temperature a) during emulsification of mineral oil using membrane with average pore size a) 0.2  $\mu\text{m}$ , b) during emulsification of mineral oil using membrane with average pore size 3 $\mu\text{m}$ , c) of lanolin, beeswax and mineral oil (with average pore size 0.2 $\mu\text{m}$ ), and d) mineral oil at different temperatures (with average pore size 0.2 $\mu\text{m}$ )

Figure 6 Image analysis results of O/W emulsions of lanolin, beeswax and mineral oil (corresponding to Figure 5a, Table 2) showing a few sample images for each size range (10-20  $\mu\text{m}$ , 5-10  $\mu\text{m}$  and < 5  $\mu\text{m}$ )

Figure 7 Volume size distribution of a) primary emulsion (W/O) made using hexadecane at room temperature, b) double emulsions of hexadecane ((W/O)/W) cooled at room temperature c) primary emulsion (W/O) made using cetyl palmitate at room temperature, d) cetyl palmitate double emulsion ((W/O)/W) samples which were initially cooled at three different temperatures e) primary emulsion (W/O) made using lanolin that was cooled at room temperature whilst stirred, f) double emulsions of lanolin ((W/O)/W) that were cooled at various conditions

Figure 8 Comparison of primary and double emulsions made using hexadecane

Figure 9 Fluorescein concentration profile over time for a) hexadecane double emulsion ((W/O)/W) cooled at three different temperatures b) cetyl palmitate double emulsion ((W/O)/W) cooled at three different temperatures, c) lanolin double emulsion ((W/O)/W) samples that were cooled at various conditions

Figure 10 Comparison of fluorescein concentration profiles over time for microcapsules of a) cetyl palmitate and hexadecane cooled at  $-26^{\circ}\text{C}$ , b) lanolin, cetyl palmitate and hexadecane, cooled at  $3^{\circ}\text{C}$ , c) for cetyl palmitate, lanolin (stirred and non-stirred) and hexadecane cooled at room temperature

Figure 11 Permeability of microcapsules of hexadecane, lanolin and cetyl palmitate against calculated microcapsules wax thickness (The line is a guide for the eye)

XME run	Organic phase		Aqueous phase		Conditions				Flux (ml(or g) /min)
	Type	Amount (net) <sup>b</sup>	Water (ml)	Surfactant (g)	Average pore size XME ( $\mu$ m)	Operating Temp ( $^{\circ}$ C)	Aqueous Flow rate (l/hr)	Duration (min)	
Castor oil	Castor oil	125 ml	1000	10.098 <sup>b</sup>	0.2	21	540	30	4.2
Coconut oil	Coconut oil	200 ml	1000	20.062 <sup>b</sup>	0.2	19	540	9	22.2
Mineral oil 1	Mineral oil	580 ml	2000	20.202 <sup>b</sup>	3	60	200	15	38.7
Mineral oil 2	Mineral oil	1250 ml	2000	20.132 <sup>b</sup>	3	80	200	7	178.6
Mineral oil 3	Mineral oil	420 ml	2000	20.043 <sup>b</sup>	0.2	60	500	43	9.8
Mineral oil 4	Mineral oil	520 ml	2500	20.900 <sup>b</sup>	0.2	80	500	20	26.0
Mineral oil 5	Mineral oil	1000 ml	4000	20 <sup>b</sup>	0.2	95	400	11	90.9
Lanolin 1	Lanolin	636 g	4000	20.07 <sup>b</sup>	0.2	60	500	61	10.4
Beeswax 1	Beeswax	924 g	4000	20.065 <sup>b</sup>	0.2	80	500	16	57.8
Double hexadecane	Single hexadecane (W/O) <sup>a</sup>	165 g	1000	47 <sup>c</sup>	0.2	20	505	180	0.9
Double cetyl palmitate	Single palmitate (W/O) <sup>a</sup>	463 g	1000	10 <sup>c</sup>	3	72	515	40	11.6
Double lanolin	Single lanolin (W/O) <sup>a</sup>	209 g	1000	20 <sup>c</sup>	3	66	500	120	1.7

Notes: a = prepared using PGPR, b = SDS; c= Tween 20

Table 1. Recipes and experimental conditions used for the primary (W/O) and double ((W/O)/W) emulsions prepared using XME.

Magnification Lens Used	Size Range ( $\mu\text{m}$ )	Number in each size range for each wax		
		Lanolin (60°C)	Beeswax (80°C)	Mineral oil (95°C)
Low Power Magnification	80-160	0	0	0
	40-80	0	1	0
	10-40	0	282	0
High Power Magnification	20-40	0	6	0
	10-20	5	66	5
	5-10	18	311	145
	<5	14876	14753	11314

Table 2 Number of emulsion droplets in each size range for O/W emulsions prepared using XME of lanolin, beeswax and mineral oil obtained using image analysis with two different lens magnifications

Material	XME conditions		Particle size distribution				Peak sizes		
	Average pore size (μm)	Operating Temperature (°C)	d(0.1) (μm)	d(0.5) (μm)	d(0.9) (μm)	Span <sup>a</sup>	Minor peak (μm)	Second Minor peak (μm)	Main peak (μm)
Hexadecane primary	--	--	3.114	9.207	18.328	1.652	3.311 shoulder	--	11.481
double	0.2	20	0.205	0.603	2.768	4.247	2.512	--	0.479
Cetyl palmitate primary	--	--	9.016	46.769	93.239	1.801	8.710	--	60.256
double -26°C	3	70	0.477	32.364	106.238	3.268	0.316	3.802	45.709
double 3°C			0.297	14.948	67.339	4.485	0.363	3.802	34.674
double rt			0.269	2.231	46.682	20.801	0.417	1.660	34.674
Lanolin primary	--	--	6.206	10.479	17.355	1.064	--	--	11.482
double rt stir	3	~60	8.819	17.257	31.768	1.33	0.275	181.970	19.953
double 3°C stir			6.053	15.171	29.202	1.526	0.275	--	17.378
double rt non-stir - top			8.88	15.839	27.113	1.151	--	--	17.378
double rt non-stir - bottom			0.509	6.912	27.817	3.951	0.275	17.378	5.012

Note: a = span is a measure of spread = (d(0.9)-d(0.1))/d(0.5)

Table 3 Size distribution results for primary (W/O) and double ((W/O)/W) emulsions of hexadecane, cetyl palmitate and lanolin prepared using XME (cooled at different temperatures)

Wax	Wax Melting point (°C)	Cooling temp (°C)	D [4, 3] - Volume weighted mean of double emulsion (µm)	Wax thickness of double emulsion (µm) <sup>a</sup>	Initial rate of fluorescein diffusion (mol dm <sup>-3</sup> min <sup>-1</sup> )		Permeability x10 <sup>-16</sup> (m <sup>2</sup> s <sup>-1</sup> )
					Rate	R <sup>2</sup>	
Hexadecane	18	-26			5.362x10 <sup>-9</sup>	0.9385	
		3			5.041x10 <sup>-9</sup>	0.5142	
		17	1.074	0.141	4.392x10 <sup>-9</sup>	0.2912	2
Lanolin	39	3 stir	16.376	2.155	1.718x10 <sup>-8</sup>	0.9244	86
		20 stir	19.666	2.588	9.804x10 <sup>-9</sup>	0.8892	59
		20 not	17.071	2.246	1.307x10 <sup>-8</sup>	0.9703	68
Cetyl Palmitate	46-51	-26	53.358	7.022	4.407x10 <sup>-8</sup>	0.9921	715
		3	28.590	3.762	3.663x10 <sup>-8</sup>	0.9876	319
		20 not	16.539	2.176	3.868x10 <sup>-8</sup>	0.9666	195
		20 stir	215.002	28.294	3.868x10 <sup>-8</sup>	0.9666	2530

Note: a= calculated from D[4,3] and known composition

cp reheated and cooled at room temp and stirred

Samples not stirred whilst cooling unless specified

Table 4 Properties of wax microcapsules prepared using primary emulsions of hexadecane, lanolin and cetyl palmitate

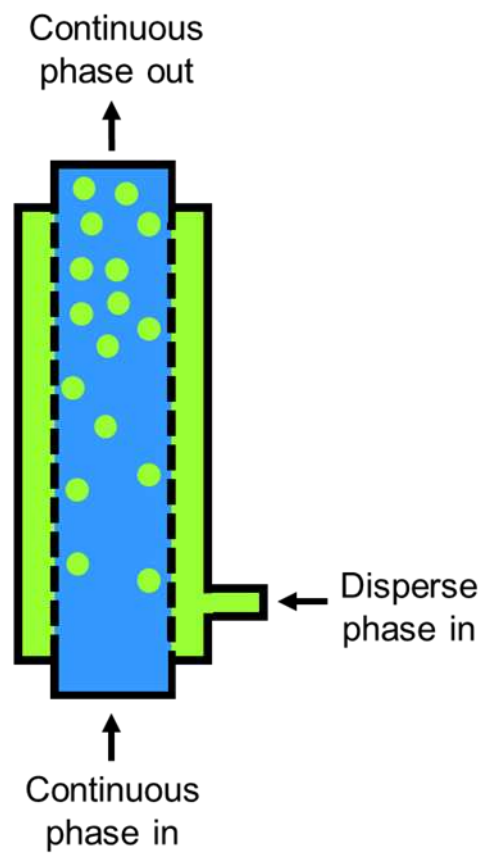


Figure 1. Schematic representation of cross flow membrane emulsification.



Figure 2. View of pilot scale XME rig from the rear, after modification (  = heated modification) where A = aqueous tank (continuous phase), O = organic phase (disperse phase), and X = XME tube

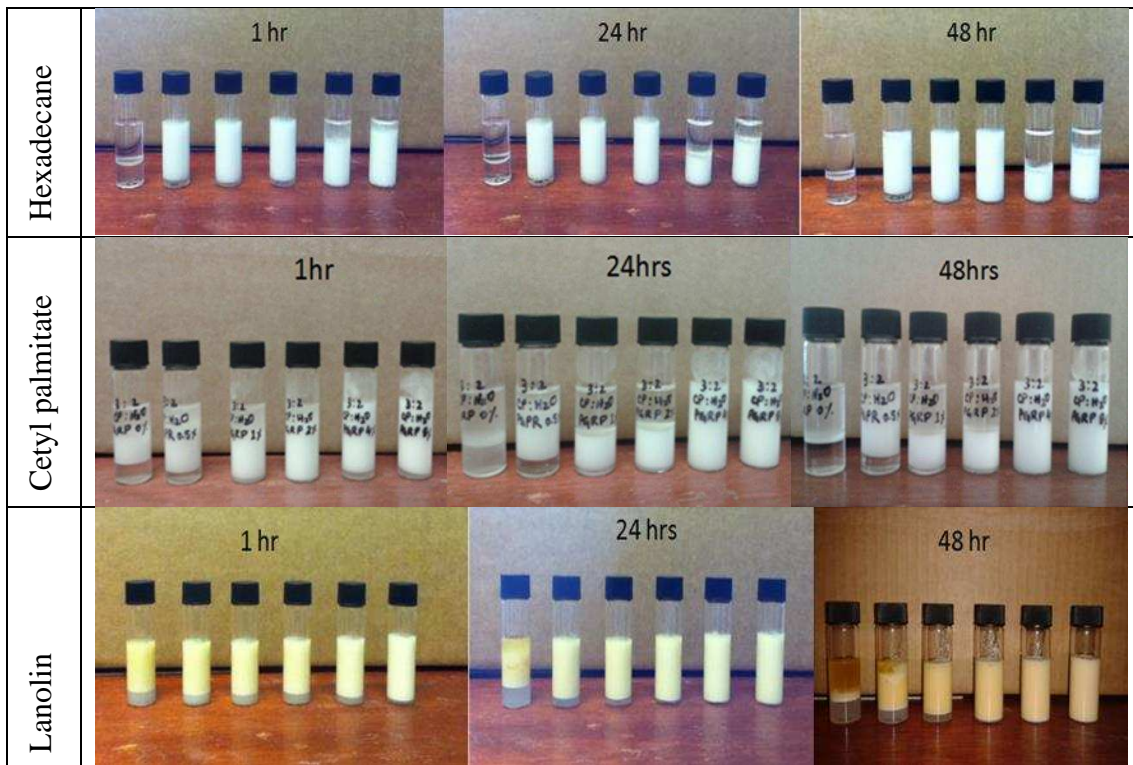


Figure 3 Photograph of primary emulsions (W/O) of oil (hexadecane, cetyl palmitate or lanolin) and water (ratio 2:3 water to oil) made using PGPR surfactant concentration of 0, 0.5, 1, 2, 4 and 8% (hexadecane and lanolin wrt oil, cetyl palmitate wrt to water) from left to right, monitored over time

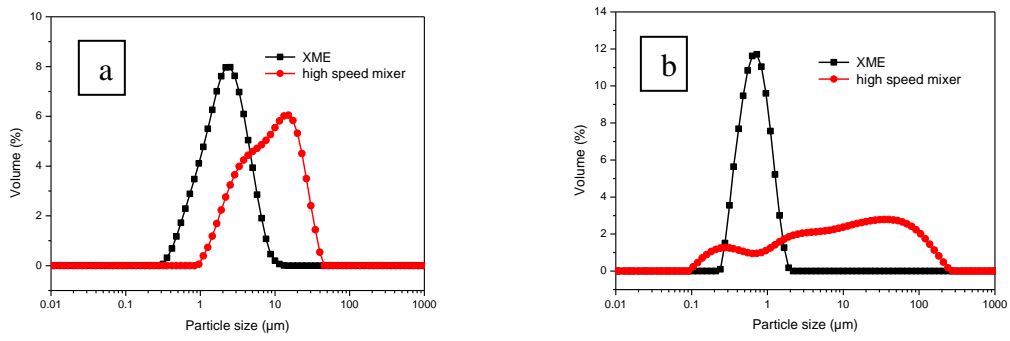


Figure 4 Volume size distributions of oil-in water emulsions made using either XME or a high speed mixer with a) coconut oil and water, and b) castor oil and water

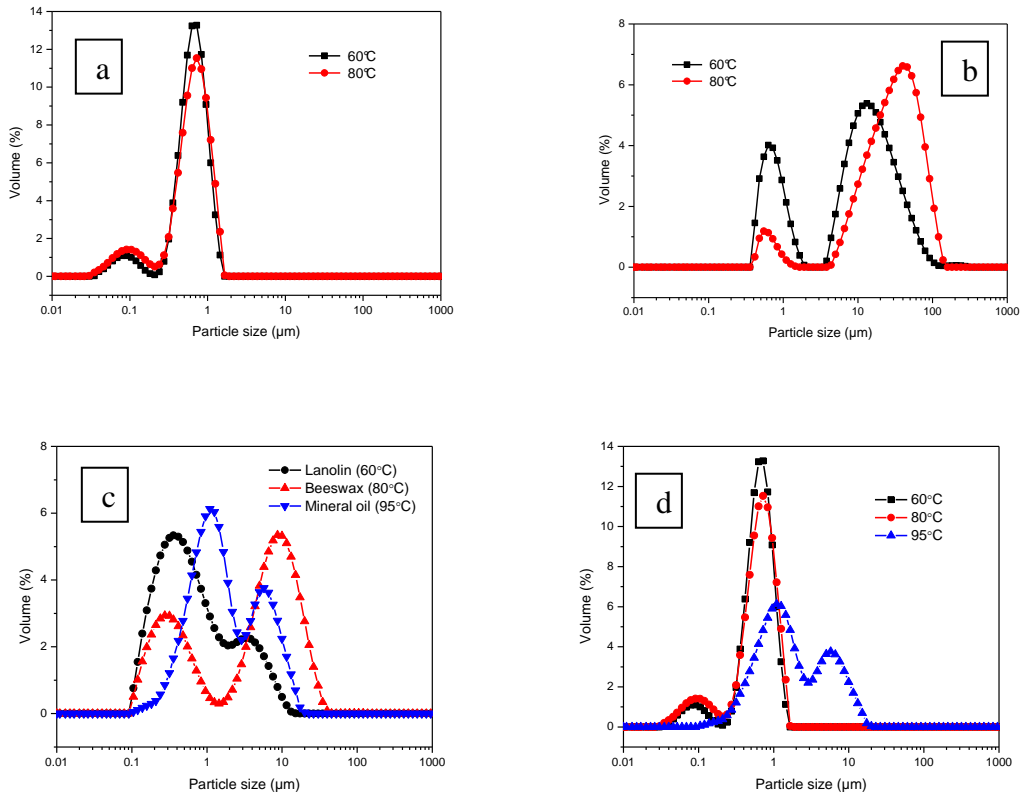


Figure 5 Volume size distribution of oil-in-water emulsions as a function of operating temperature a) during emulsification of mineral oil using membrane with average pore size a) 0.2 μm, b) during emulsification of mineral oil using membrane with average pore size 3 μm, c) of lanolin, beeswax and mineral oil (with average pore size 0.2 μm), and d) mineral oil at different temperatures (with average pore size 0.2 μm)

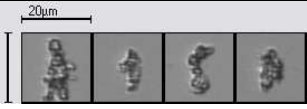
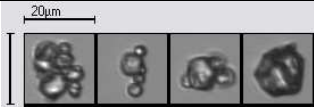
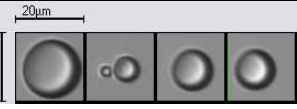
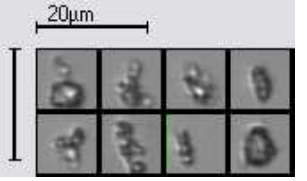
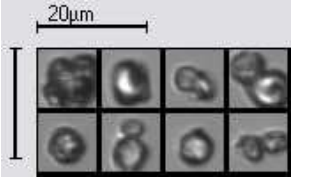
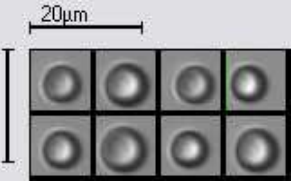
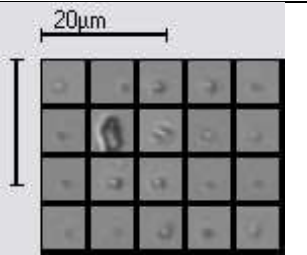
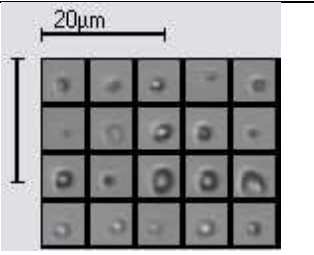
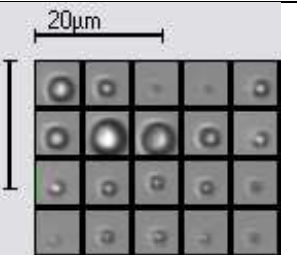
Size Range ( $\mu\text{m}$ )	Lanolin	Beeswax	Mineral oil
10-20			
5-10			
<5			

Figure 6 Image analysis results of O/W emulsions of lanolin, beeswax and mineral oil (corresponding to Figure 4c, Table 2) showing a few sample images for each size range (10-20  $\mu\text{m}$ , 5-10  $\mu\text{m}$  and < 5  $\mu\text{m}$ )

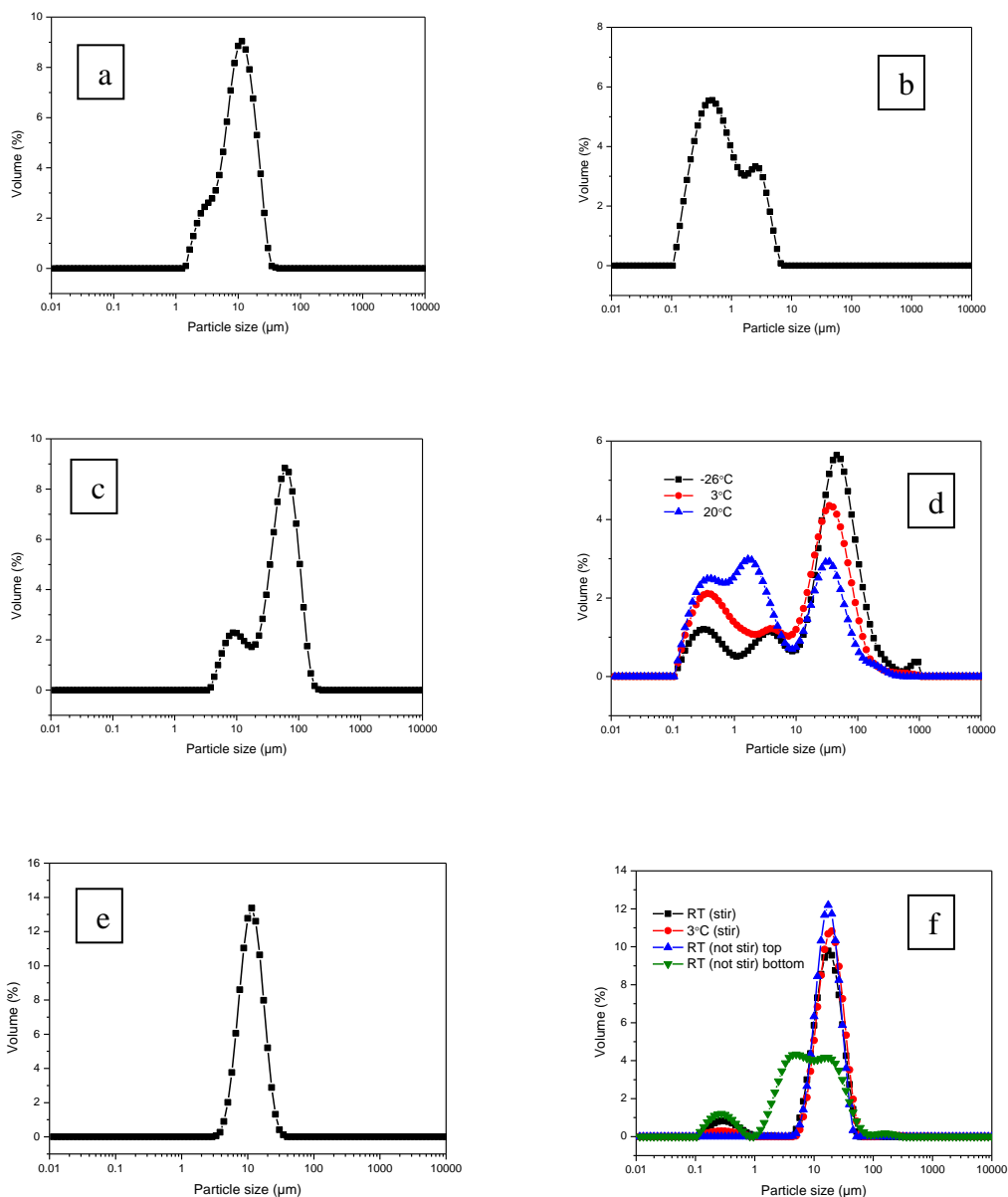


Figure 7 Volume size distribution of a) primary emulsion (W/O) made using hexadecane at room temperature, b) double emulsions of hexadecane ((W/O)/W) cooled at room temperature c) primary emulsion (W/O) made using cetyl palmitate at room temperature, d) cetyl palmitate double emulsion ((W/O)/W) samples which were initially cooled at three different temperatures e) primary emulsion (W/O) made using lanolin that was cooled at room temperature whilst stirred, f) double emulsions of lanolin ((W/O)/W) that were cooled at various conditions



Figure 8 Comparison of primary and double emulsions made using hexadecane

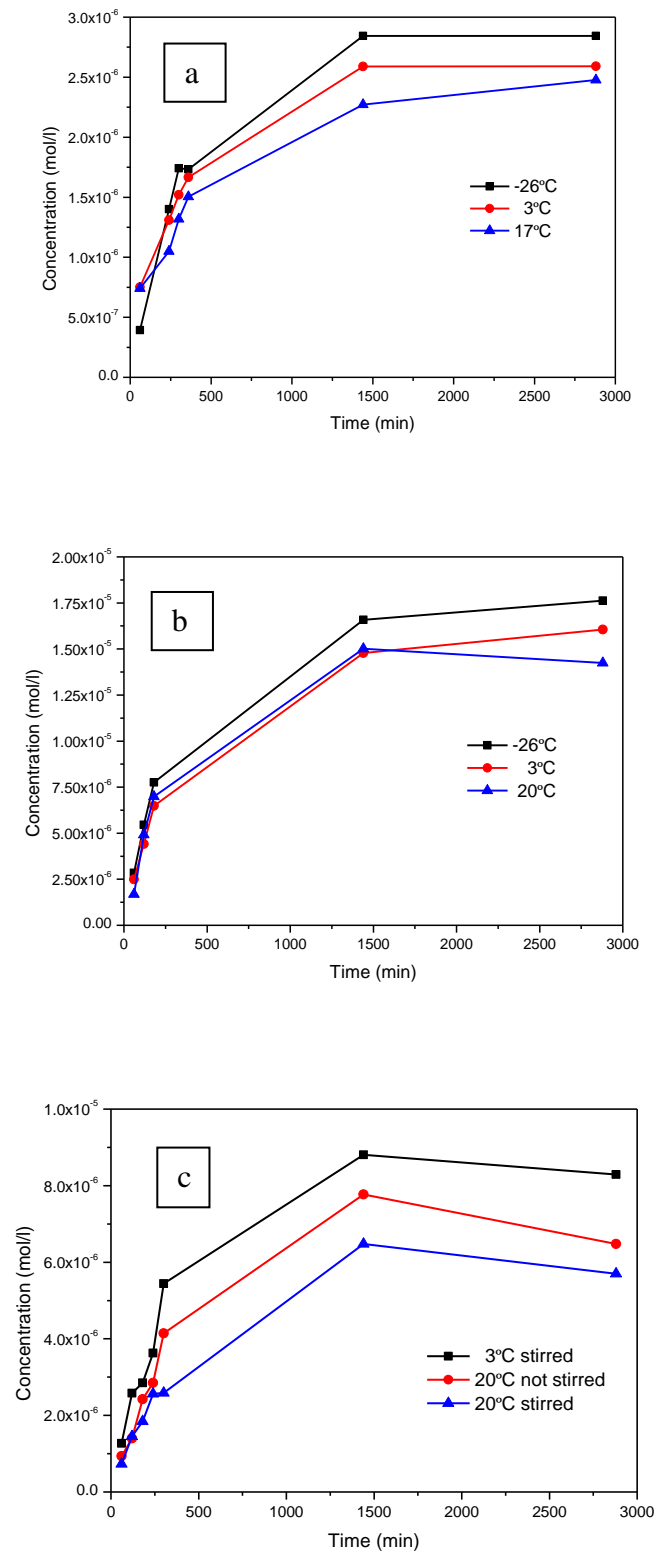


Figure 9 Fluorescein concentration profile over time for a) hexadecane double emulsion ((W/O)/W) cooled at three different temperatures b) cetyl palmitate double emulsion

((W/O)/W) cooled at three different temperatures, c) lanolin double emulsion ((W/O)/W) samples that were cooled at various conditions

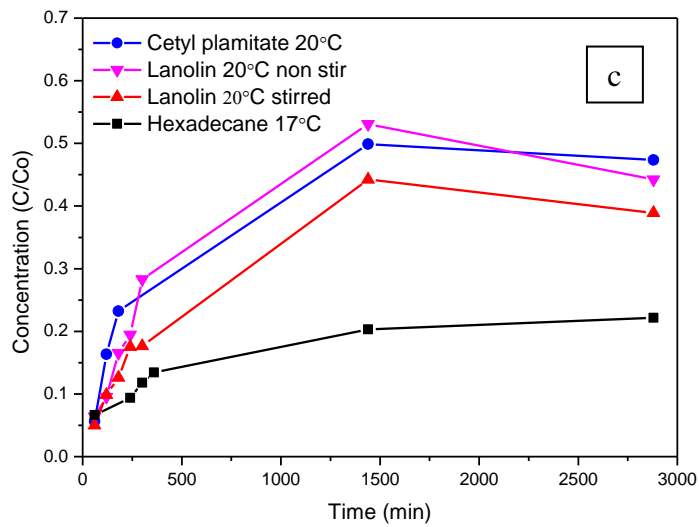
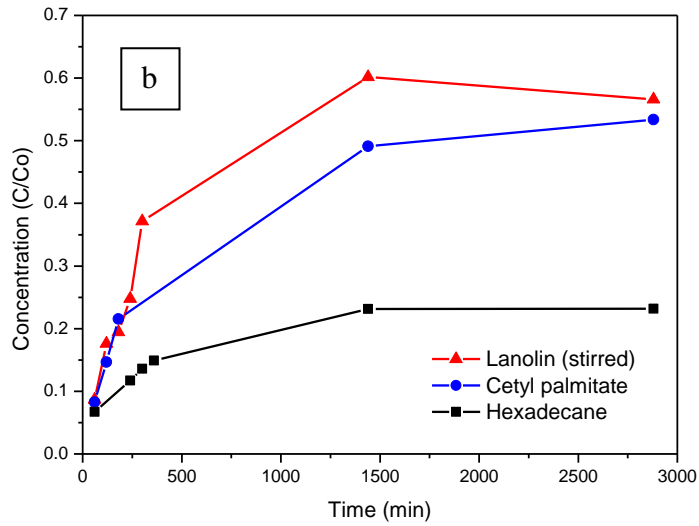
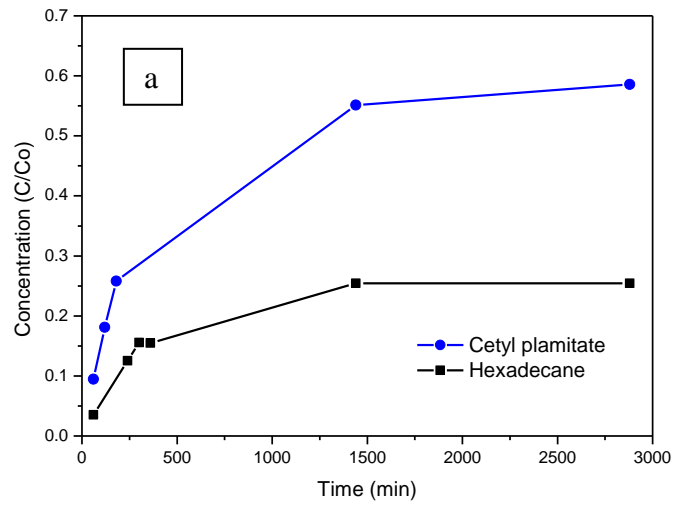


Figure 10 Comparison of fluorescein concentration profiles over time for microcapsules of a) cetyl palmitate and hexadecane cooled at  $-26^{\circ}\text{C}$ , b) lanolin, cetyl palmitate and hexadecane, cooled at  $3^{\circ}\text{C}$ , c) for cetyl palmitate, lanolin (stirred and non-stirred) and hexadecane cooled at room temperature

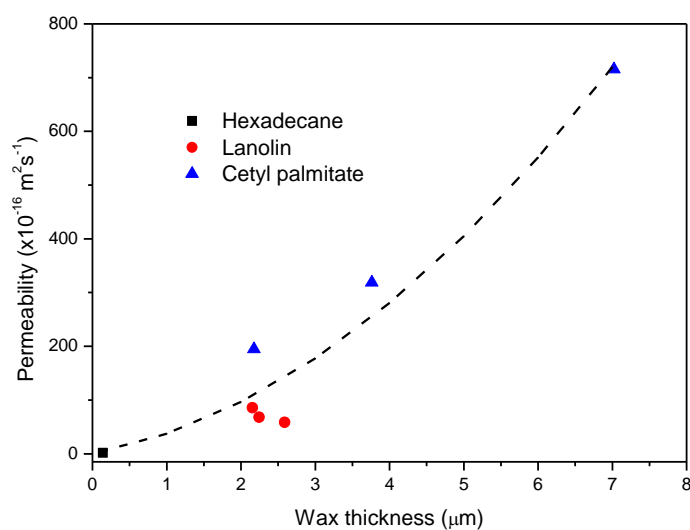


Figure 11 Permeability of microcapsules of hexadecane, lanolin and cetyl palmitate against calculated microcapsules wax thickness (The line is a guide for the eye)